Supplemental information for: "Continuous illumination picosecond imaging using a delay line detector in a transmission electron microscope"

Teresa Weßels,[1,2] Simon Däster,[3] Yoshie Murooka,[1] Benjamin Zingsem,[4] Vadim Migunov,[1,5] Maximilian Kruth,[1] Simone Finizio,[6] Peng-Han Lu,[1] András Kovács,[1] Andreas Oelsner,[7] Knut Müller-Caspary,[1,8] Yves Acremann,[3] and Rafal E. Dunin-Borkowski[1]

[1] *Ernst Ruska-Centre for Microscopy and Spectroscopy with Electrons and Peter Grünberg Institute, Forschungszentrum Jülich, 52425 Jülich, Germany*
[2] *Lehrstuhl für Experimentalphysik IV E, RWTH Aachen University, 52056 Aachen, Germany*
[3] *Laboratory for Solid State Physics, ETH Zurich, 8093 Zurich, Switzerland*
[4] *Faculty of Physics and Center for Nanointegration (CENIDE), University of Duisburg-Essen, 47057 Duisburg, Germany*
[5] *Central Facility for Electron Microscopy (GFE), RWTH Aachen University, 52074 Aachen, Germany*
[6] *Swiss Light Source, Paul Scherrer Institut, 5232 Villigen PSI, Switzerland*
[7] *Surface Concept GmbH, 55124 Mainz, Germany*
[8] *Department of Chemistry, Ludwig-Maximilians-Universität München, Butenandtstrasse 5-13, 81377 Munich, Germany*

1. VIDEOS OF MAGNETIC VORTEX CORE GYRATION

Videos of magnetic vortex core gyration at 414, 417, 419, 421, 424, and 450 MHz are available as additional Supplementary Material. They show largely unprocessed data, in which only the contrast has been adjusted to make the magnetic vortex core visible.

2. ESTIMATION OF MICROWAVE MAGNETIC FIELD

The strength of the microwave magnetic fields was estimated based on its interaction with the electron beam. The deflection of the electrons due to this interaction was imaged using low angle diffraction on a standard charge-coupled device camera [1]. The deflection angle θ can be correlated to the applied field $B_\perp$ *via* the expression

$$\theta = \frac{e\lambda}{h} B_\perp t \quad , \tag{1}$$

where e is the electron charge, $\lambda = 2\,\mathrm{pm}$ is the electron wavelength at an accelerating voltage of 300 kV and h is Planck's constant [2]. The thickness t of the cartridge is $\sim$500 μm. The deflection is measured to be 16 μrad for an applied RF current at 418 MHz and 23 dBm (see Fig. 1). Hence, the magnetic field is estimated to be $\sim$0.07 mT. The presence of a bright spot in Fig. 1 results from a part of the RF current being reflected back to the frequency generator and the generator turns off for a short time. During this time no microwave fields are applied and the electron beam is located at the center. In contrast to the magnetic fields, a deflection due to the induced electric fields is not expected as the holder is designed in such a way that they are aligned parallel to the electron beam direction [3]. The absence of in-plane electric fields is experimentally confirmed by the pure linear deflection of the electron beam due to the microwave fields imaged with LAD (see Fig. 1).

When applying Eq. 1, it is assumed that the magnetic field in the cartridge is uniform and that there are no stray fields. Both assumptions are likely to result in an underestimation of the magnetic field, since it is strongest at the sample position. There are likely to be stray fields outside of the cartridge that deflect the electron beam in the opposite direction than the fields in the cartridge. Although the field depends on applied frequency, it does not change strongly over the frequency range of the magnetic vortex core gyration, since the resonant frequency is constrained to a small range.

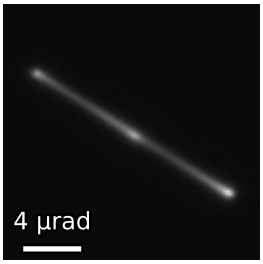

FIG. 1: Deflection of the electron beam due to a microwave magnetic field at 418 MHz and 23 dBm applied power imaged using low angle diffraction on a charge-coupled device camera. The bright spot in the center results from reflection of the RF current into the RF generator.

3. INTERACTION OF THE MICROWAVE FIELD AND THE ELECTRON BEAM

Due to the Lorentz force, the microwave field does not only interact with the sample, but also with the electron beam itself. The magnetic microwave field therefore creates an image shift out of focus (see Fig. 2a). As the microwave excitation is sinusoidal, the deflection also takes on a sinusoidal shape. This knowledge can be used to correct for the image shift, according to the equation

$$\begin{aligned} y_1 &= y_0 + y' \\ y_0 &= y_1 - y' = y_1 - [a \cdot sin(b \cdot t + c) + d] \quad , \end{aligned} \tag{2}$$

where it is assumed for simplicity that the beam is purely deflected along the y axis. The deflected coordinate y_1 can be obtained by adding the deflection y' to the non-deflected coordinate y_0. The parameter a corresponds to the amplitude of the deflection. The remaining parameters are required to match the phase and offset.

The parameters needed for correction were determined by using the following procedure:

1. The dataset at 450 MHz was assumed to be out of resonance, with the magnetic vortex core stationary in the disk. The movement of the core in the images was then assumed to be purely due to the electron beam interaction. After rotating the image so that the primary axis of motion was along the y axis, a sinusodial function was fitted to the dependence of the magnetic vortex core position on time. This fit provided the beam deflection y'. When subtracting it from the experimental dataset, one can obtain the parameter y_0. The amplitude of the beam shift is used to determine the shift for all other frequencies and corresponds to the parameter a in Eq. 2. The parameters b, c and d are needed to match the phase in the excitation cycle. Figure 2b shows the correction for the deflection at 450 MHz.

2. In the next step, the magnetic vortex core movement at different frequencies was studied. Each dataset was rotated so that the primary movement followed the y axis by using the rotation angle determined for 450 MHz. Sinusoidal functions were fitted to them to determine the parameters b, c and d to match the phase and offset. In this way, all of the parameters describing the beam deflection due to the microwave-beam interaction could be determined.

In the final step, the image shift due to interaction of the microwave and the electron beam was removed from every dataset by subtracting image shift from the movement of the magnetic vortex core using the amplitude a of the interaction determined at 450 MHz and the phase parameters b, c and d determined at each frequency.

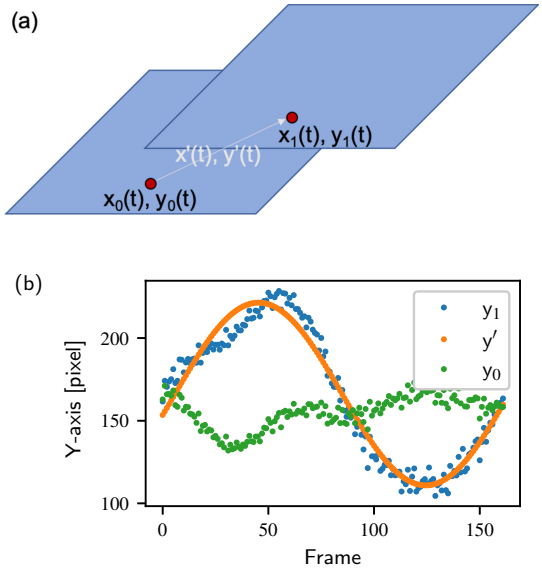

FIG. 2: Interaction of the microwave field and the electron beam. (a) Visualization of image shift due to the microwave field. The image is shifted depending on the phase of the excitation cycle and follows a sinusoidal motion. The position of the disk is marked in red and does not change in the image. However, its position shifts with the image and therefore also follows a sinusoidal motion. (b) Correction of image shift introduced by the microwave field of the holder. The blue dots represent the measured position of the vortex core. The orange dots show a sinusoid fitted to this motion. The green dots show motion of the magnetic vortex core after subtraction of the sinusoid.

4. IMAGE DISTORTIONS

Images recorded using the DLD were distorted due to issues with the control electronics of the imaging filter. As a result, straight lines in the images appeared bent, as shown in an image of a standard calibration sample with a lattice spacing of ∼480 nm in Fig. 3a. In addition to distortions, it was not possible to illuminate the full area of the DLD. These image distortions were corrected applying the Brown-Conrady model [4] which can take tangential as well as radial distortions into account. Figure 3b shows the image of the calibration sample after distortion correction. Even though the distortions were not fully removed, the degree of bending is reduced.

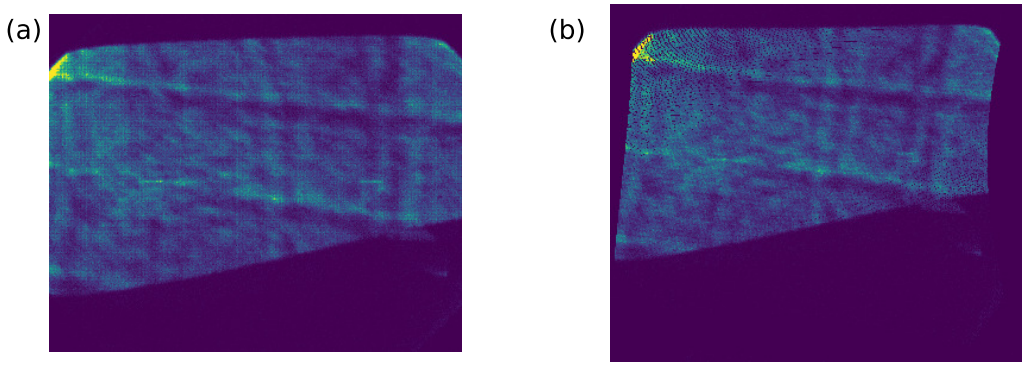

FIG. 3: Image of a calibration sample with a periodic lattice spacing. (a) Original image revealing distortion of the image due to electronic issues. (b) Calibration sample after correction of image distortions.

[1] F. Goncalves, G. Paterson, D. McGrouther, T. Drysdale, Y. Togawa, D. Schmool, and R. Stamps, *Probing microwave fields and enabling in-situ experiments in a transmission electron microscope*, Scientific reports **7**, 1 (2017).
[2] A. Kovács and R. E. Dunin-Borkowski, in *Handbook of Magnetic Materials*, Vol. 27 (Elsevier, 2018) pp. 59–153.
[3] B. Zingsem, *Pico-second spin dynamics in nano-structures: Towards nanometer spatial resolution by Transmission electron microscopy*, Ph.D. thesis, Universität Duisburg-Essen (2020).
[4] C. Brown, *Close range camera calibration, symposium on close range photogrammetry*, Photogramm. Eng. Remote. Sens. **8**, 855–866 (1971).